

## XAFS of the P K-edge in the soft magnetic $\text{Fe}_{85.2}\text{Si}_1\text{B}_9\text{P}_4\text{Cu}_{0.8}$ alloy exhibiting ultra-low core loss

Makoto Matsuura<sup>\*1</sup>, Masahiko Nishijima<sup>1</sup>, Kazuya Konno<sup>2</sup>, Kana Takenaka<sup>1</sup> and Akihiro Makino<sup>1</sup>  
<sup>1</sup> Research and Development Center for Ultra High Efficiency Nano-crystalline Soft Magnetic Material, Institute for Materials Research, Tohoku University, Sendai, Miyagi, 980-8577, Japan  
<sup>2</sup> Sendai National College of Technology, Nodayama, Medeshima, Natori 982-1239, Japan

XAFS measurements of the P K-edge for the soft magnetic  $\text{Fe}_{85.2}\text{Si}_1\text{B}_9\text{P}_4\text{Cu}_{0.8}$  alloy with ultra-low core loss were carried out using a total electron yield in the course of nanocrystallization of bcc iron. Results of the XANES and EXAFS show that surface oxidation of P evolves during thermal annealing. Although XANES spectra show that a very small amount of P atoms can be accompanied with precipitated bcc Fe nanocrystallites, EXAFS results indicate that a major part of P atoms are excluded from bcc iron nanocrystallites and remained in the residual amorphous phase.

### 1 Introduction

Nanocrystalline Fe-based soft-magnetic alloys have been attracted much attention because of their extremely low core loss. One of the most successful nanocrystalline soft-magnetic alloys is FINEMET<sup>®</sup> which has been applied to electronic devices, such as inductors and high frequency transformers [1]. Recently a new nanocrystalline Fe-based  $\text{Fe}_{85}\text{Si}_2\text{B}_8\text{P}_4\text{Cu}_1$  soft magnetic alloy (NANOMET<sup>®</sup>) has been developed by Makino *et al.* [2]-[4]. NANOMET has excellent soft magnetic properties; low coercivity ( $H_c \sim 5.8$  A/m) and high saturation magnetic flux density ( $B_s \sim 1.82$  T). It is quite important to elucidate the nanocrystallization kinetics of NANOMET. Like as FINEMET small additives of Si, Cu and P in NANOMET play essential role on nanocrystallization. Nanocrystallization kinetics of NANOMET may be quite different from FINEMET because of different concentration; higher Fe (73.5→85 at%), lower Si (13.5→2 at%) and no Nb but P is included. In the previous works the authors reported roles of Cu in nanocrystallization of NANOMET by X-ray absorption fine structure (XAFS) [5], [6]. In this work the local structure around P in NANOMET are measured to elucidate the role of P in the nanocrystallization kinetics of NANOMET by means of XAFS.

### 2 Experiments and data analyses

Sample of  $\text{Fe}_{85.2}\text{Si}_1\text{B}_9\text{P}_4\text{Cu}_{0.8}$  was prepared by a single roller melt-spinning technique in air. Thickness and width of the ribbons are 16  $\mu\text{m}$  and 5 mm, respectively. Annealing of the as-quenched (as-Q) samples was done in a differential scanning calorimetry (DSC) apparatus (Perkin-Elmer DSC 8000) at a heating rate of 300 K/min under a flow of Ar gas. The high heating rate of 300 K/min in the annealing is adopted to obtain nanocrystalline bcc Fe in the  $\text{Fe}_{85.2}\text{Si}_1\text{B}_9\text{P}_4\text{Cu}_{0.8}$  alloy. The samples prepared for the XAFS measurements were those: as-Q, annealed at 340°C for 0 s, 420 °C for 600 s and 650 °C for 0 s. From X-ray diffraction and transmission microscopy measurements it is known that the as-quenched amorphous  $\text{Fe}_{85.2}\text{Si}_1\text{B}_9\text{P}_4\text{Cu}_{0.8}$  alloy exhibits two crystallization steps by annealing; bcc-Fe

precipitation at 434 °C ( $T_{x1}$ ) and Fe-(B,P) compounds formation at 571 °C ( $T_{x2}$ ) [6]. The sample annealed at 420 °C for 600 s has homogeneously distributed bcc-Fe nanocrystallites,  $\sim 12$  nm in grain size, and exhibits the optimum soft-magnetic properties.

A crystalline  $\text{Fe}_{99}\text{P}_1$  alloy was prepared as a reference material by water-quenching an arc-melted ingot after annealed at 1100 °C for 10 hours. XAFS measurements of the P K-edge absorption ( $E_0=2145.5$  eV) were carried out at BL11B by a total electron yield (TEY) method at room temperature. The acquired raw data is manipulated using a program Athena [7] to reduce EXAFS functions  $\chi(k)$  and their Fourier transformation  $F(r)$ . Program FEFF9 [8] was used to simulate a XANES spectrum of P in bcc Fe and EXAFS spectra of P in  $\text{P}_2\text{O}_5$  and Fe-(B,P) compounds.

### 3 Results and Discussion

#### 3-1 XANES results

Figure 1 shows XANES spectrum of the P K-edge for the  $\text{Fe}_{99}\text{P}_1$  alloy together with a simulated result of a P in bcc iron using FEFF9, where P atom is put at a substitutional site of bcc iron. In Fig. 1 the energy of the

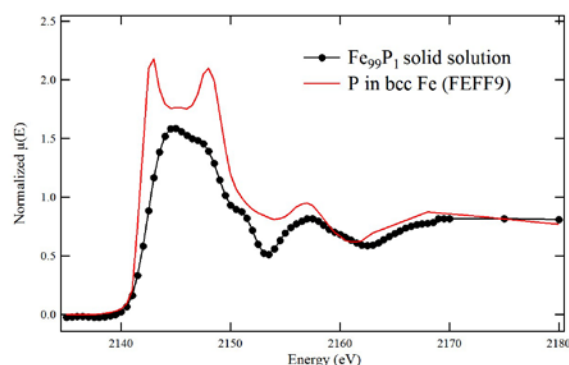


Figure 1 XANES spectra of the P K-edge for the  $\text{Fe}_{99}\text{P}_1$  alloy super-saturated with P in bcc Fe together with the calculated result of P occupied a substitutionally site of bcc Fe using FEFF9.

simulated result is shifted by -7 eV to fit with absorption edge of the experiment. Because the  $\text{Fe}_{99}\text{P}_1$  alloy sample is a super saturated solid solution of P in bcc Fe, P atoms in this alloy are expected to occupy either substitutional or interstitial sites of bcc iron. Although the calculated result does not well agree with the experiments as shown in Fig.1, it represents the experimental result as a whole. The contamination of sulfur in the sample prevents to extract a reliable EXAFS function  $\chi(k)$ . Therefore we can't determine in which site P occupies: either substitutional or interstitial site of bcc iron. Figure 2 shows XANES spectra of the P K-edge for the  $\text{Fe}_{85.2}\text{Si}_1\text{B}_9\text{P}_4\text{Cu}_{0.8}$  alloy of the as-quenched, annealed at 340 °C, 650 °C for 0 s and 420 °C for 600 s together with those of the  $\text{Fe}_{99}\text{P}_1$  solid solution and  $\text{K}_3\text{PO}_4$ .  $\text{K}_3\text{PO}_4$  is adopted as a typical XANES spectrum of an oxidized state of phosphorous. Two characteristic peaks indicated as A and B in Fig. 2 develop during the annealing. The peak A corresponds to a shoulder of  $\text{Fe}_{99}\text{P}_1$  solid solution and then a slight increase of the peak A indicates the increase in the number of P in bcc iron with annealing temperature. On the other hand the peak B in Fig. 2 agrees with that of the  $\text{K}_3\text{PO}_4$ . Simulated results of the EXAFS of P in  $\text{P}_2\text{O}_5$  also show the development of the oxidation of P as described below. Therefore, increase in the intensity of a peak B means that a degree of surface oxidation develops with annealing temperature and time. The maximum intensity of the peak B was found in the annealed at 420 °C for 600 s.

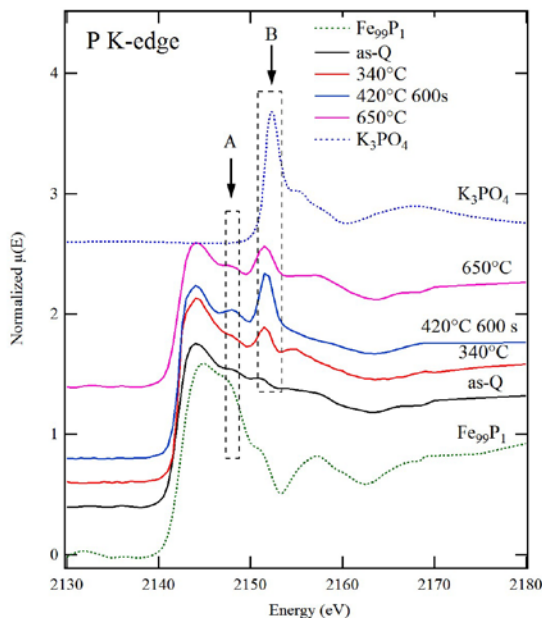


Figure 2 XANES spectra of the P K-edge for the  $\text{Fe}_{85.2}\text{Si}_1\text{B}_9\text{P}_4\text{Cu}_{0.8}$  alloy, as-Q, annealed at 340 °C, 420 °C and 650 °C, together with those of the  $\text{Fe}_{99}\text{P}_1$  alloy and  $\text{K}_3\text{PO}_4$ .

### 3-2 EXAFS results

Figures 3(a) and 3(b) show results of EXAFS function  $k\chi(k)$  of the P K-edge and their magnitude of the

Fourier transform, respectively, for the  $\text{Fe}_{85.2}\text{Si}_1\text{B}_9\text{P}_4\text{Cu}_{0.8}$  alloy of the as-quenched, annealed at 340 °C, 650 °C for 0 s and 420 °C for 600 s. Fourier transform was achieved in the range of  $3 < k < 10 \text{ \AA}^{-1}$ . A fairly small effect of contamination of sulfur is recognized in the region of  $k \sim 9.4 \text{ \AA}^{-1}$  shown by a dotted line. Results of the Fourier transform shown in Fig. 3(b) indicate that the height of the first peak of the as-Q sample decreases at 420 °C, whereas increase at 650 °C. It is probably due to the fact

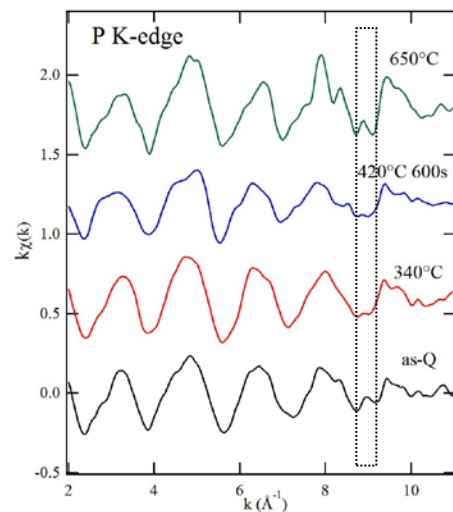


Figure 3(a) EXAFS results of the P K-edge for the  $\text{Fe}_{85.2}\text{Si}_1\text{B}_9\text{P}_4\text{Cu}_{0.8}$  alloy; as-Q, annealed at 340 °C, 420 °C and 650 °C.

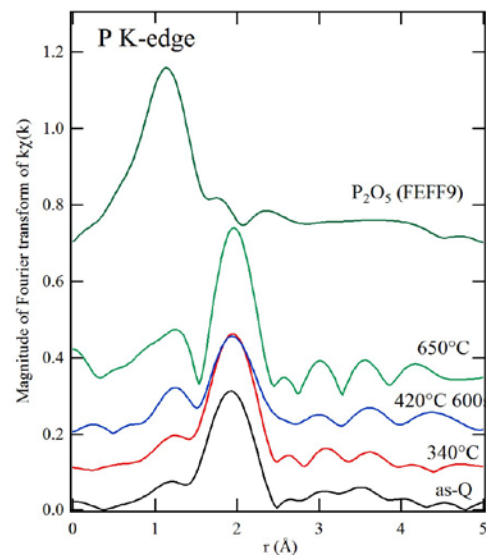


Figure 3(b) Magnitude of the Fourier transform of  $k\chi(k)$  for the  $\text{Fe}_{85.2}\text{Si}_1\text{B}_9\text{P}_4\text{Cu}_{0.8}$  alloy; as-Q, annealed at 340 °C, 420 °C and 650 °C together with that of the calculated  $\text{P}_2\text{O}_5$  using FEFF9.

that P is excluded from the precipitated bcc Fe nanocrystallites due to a negligible solubility of P in iron

and then P is enriched in the residual amorphous region, where concentration ratio of P/Fe is much higher than the as-quenched amorphous state. The prominent change of the radial structure function shown in Fig. 3(b) is an increase in the intensity of the peak at around 1.2 Å with annealing temperature.

In order to characterize this peak, simulation of the P K-edge EXAFS for  $P_2O_5$  was done using FEFF9 and result is shown in Fig. 3(b). The calculated result of the  $P_2O_5$  suggests that peak at around 1.2 Å can be attributed to the phosphorus oxide. Therefore, the increase in the intensity of this peak with annealing temperature indicates that oxidation of P develops with annealing temperature.

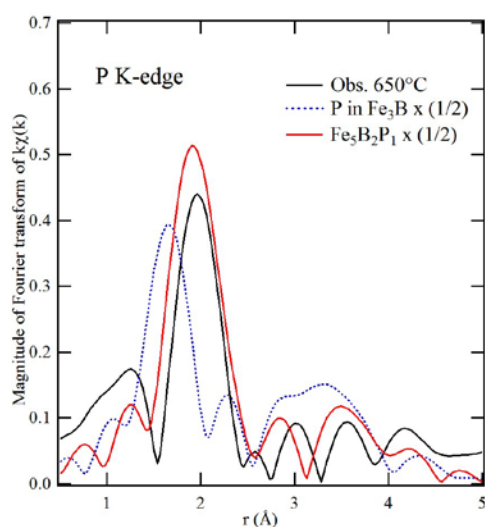


Figure 4 Magnitude of Fourier transform of the  $k\chi(k)$  of the P K-edge for the  $Fe_{85.2}Si_1B_9P_4Cu_{0.8}$  alloy annealed at 650 °C and simulated results of P in  $Fe_3B$  and  $Fe_5B_2P_1$  compounds.

TEM observation shows that P is excluded from the precipitated bcc Fe into a residual amorphous phase for the sample annealed at 420 °C for 600 s [5]. The residual amorphous phase crystallizes at 571 °C into Fe-(B,P) compounds. High energy X-ray diffraction identified such Fe(B,P) compounds as  $Fe_3(P_{0.37}B_{0.63})$  and  $Fe_{15}Si_3B_2$  [9]. We simulated an EXAFS function  $\chi(k)$  of P in the  $Fe_3B$  and  $Fe_5B_2P_1$  compounds using FEFF9; their structure type and space group are  $Fe_3C$  (Pnma) and  $Cr_5B_3$  (I4/mcm), respectively. In the simulation of the  $Fe_3B$  compound, a central absorbing P atom is substituted for a B atom in  $Fe_3B$ . Figure 4 shows the simulated results of the magnitude of Fourier transform of the P K-edge for two compounds and the observed results for the annealed at 650 °C. The results show that P in  $Fe_5B_2P_1$  is much better representable to the observed data than P in  $Fe_3B$  compound.

#### Discussion

Results of the P-Kedge EXAFS for the  $Fe_{85.2}Si_1B_9P_4Cu_{0.8}$  show a quite different behavior during nanocrystallization process from those of the Cu and Fe K-edge; the first coordination peak increases sharply at or just below  $T_{x1}$  for the cases of Cu and Fe, whereas it does not increase or even decreases just above  $T_{x1}$  for P. This fact clearly indicates that although a very small amount of P is included in the precipitated bcc Fe as shown in the XANES spectra, most of P atoms are rejected from nanocrystalline bcc Fe and pile up in the residual amorphous phase. At present a precise analysis of local structure around P in the  $Fe_{85.2}Si_1B_9P_4Cu_{0.8}$  alloy during nanocrystallization is difficult. It is because that EXAFS amplitude does not show significant change from disordered state, i.e. amorphous state, even above the second crystallization temperature. Furthermore, surface oxidization of P precludes a precise analysis. To overcome the above problems two measurements are necessary; one is that a fluorescence method rather than a TEY should be used to lower the surface sensitivity. Another is that a low temperature XAFS measurement is preferable to suppress thermal fluctuation of P atoms. For the sake of it ultra-high vacuum system is necessary to avoid a surface contamination of S or Cl included in air.

#### Acknowledgement

The authors would like to acknowledge many thanks to Prof. Y. Kitajima for the help of XAFS measurements at BL11B in Photon Factory and for the valuable discussion. This work was financially supported by Ministry of Education, Culture, Sports, Science and Technology (MEXT), Japan under "Tohoku Innovative Materials Technology Initiatives for Reconstruction" project, "Ultra-low Core Loss Magnetic Material Technology Area.

#### References

1. Y. Yoshizawa, S. Oguma, and K. Yamauchi, *J. Appl. Phys.* 64, 6044(1988).
2. A. Makino, T. Kubota, K. Yubuta, A. Inoue, A. Urata, K. Matsumoto, and S. Yoshida, *J. Apply. Phys.* 109, 07A302-1(2011).
3. A. Makino, H. Men, T. Kubota, K. Yubuta, and A. Inoue, *Mater. Trans.* 50, 204(2009).
4. A. Makino, *IEEE Trans. Magn.* 48, 1331(2012).
5. M. Nishijima, M. Matsuura, Y. Zhang, K. Takenaka, and A. Makino, *IEEE Trans. Mag.* 50, 2004004(2014).
6. M. Nishijima, M. Matsuura, K. Takenaka, A. Takeuchi, H. Ofuchi, and A. Makino, *AIP Advances*, 4, 057129(2014).
7. B. Ravel and M. Newville, *J. Synch. Rad.* 12, 537(2005).
8. J. J. Rehr, J. J. Kas, F. D. Vila, M. P. Prange, K. Jorissen, *Phys. Chem. Chem. Phys.*, 12, 5505(2010).
9. M. Nishijima, M. Matsuura, K. Takenaka, A. Makino, to be published.

\* m\_matsuura@imr.tohoku.ac.jp